

## Two Crossovers in the Pseudogap Regime of $\text{YBa}_2\text{Cu}_3\text{O}_{7-\delta}$ Superconductors Observed by Ultrafast Spectroscopy

O. V. Misochko,<sup>1,2</sup> N. Georgiev,<sup>1</sup> T. Dekorsy,<sup>1</sup> and M. Helm<sup>1</sup>

<sup>1</sup>*Institute for Ion Beam Physics and Materials Research, Research Center Rossendorf, P.O. Box 510119, D-01314 Dresden, Germany*

<sup>2</sup>*Institute of Solid State Physics, Russian Academy of Sciences, 142432 Chernogolovka, Moscow region, Russia*

(Received 7 December 2001; published 22 July 2002)

We have investigated the temperature dependence of the optical reflectivity on a femtosecond scale in a near optimally doped  $\text{YBa}_2\text{Cu}_3\text{O}_{7-\delta}$  superconductor. The combined study of the lattice and carrier dynamics at temperatures above  $T_c$  allows us to identify two crossover temperatures in the normal state, giving evidence for an inhomogeneity of the pseudogap regime. These crossovers exhibit a clear hysteresis behavior depending on the direction of temperature change. The carrier and lattice dynamics within the crossover regimes show distinct differences from and similarities to the superconducting state, which may help in choosing between the competing theories for the pseudogap state.

DOI: 10.1103/PhysRevLett.89.067002

PACS numbers: 74.72.Bk, 74.25.Kc, 74.76.Bz, 78.47.+p

One of the main difficulties in the understanding of the microscopic mechanism of high- $T_c$  superconductivity is related to the very unusual normal (nonsuperconducting) properties of these complex materials. There are numerous normal state anomalies observed by a number of spectroscopic techniques such as infrared, Raman, and angle-resolved photoemission spectroscopy, and there is no theoretical consensus about their origin [1]. These anomalies are thought to arise from a pseudogap state that, depending on the carrier concentration, is realized below a certain temperature  $T^* \geq T_c$ . All of these anomalies evidence that superconductivity does not disappear completely at  $T_c$ , but there exists a temperature range where some of the superconducting properties persist even above  $T_c$ . There are two basic scenarios for explaining the pseudogap anomalies. The first one is based on preformed electron pairs with the subsequent establishment of their phase coherence below  $T_c$ . The second scenario suggests that the pseudogap state emerges due to short-range order fluctuations of the dielectric type (antiferromagnetic, charge-density-wave, phase separation on a microscopical scale, etc.). Most theoretical models consider the pseudogap regime as uniform, whose width ( $T^* - T_c$ ) in the phase diagram depends on the doping level. This width is maximal for underdoped compositions shrinking to zero at a doping level slightly higher than optimal. However, a few theoretical studies suggest that there is a crossover within the pseudogap state making the state nonuniform and split into two regimes characterized by distinct dynamical and relaxational properties [2–4]. Though in recent years enormous progress in clarifying the properties of the pseudogap state including its symmetry was made, many problems remain open yet [1]. This is related in part to the fact that the energy scales characteristic of superconducting and pseudogap states are very close, which, coupled to the fact that the symmetry of the two gaps seems to be the same, makes it extremely difficult to distinguish them. Although not yet employed as exten-

sively as the above-mentioned spectroscopic studies, time-domain spectroscopy can potentially delineate which electronic states are responsible for the superconductivity and what is the connection, if any, of the pseudogap above  $T_c$  with the superconducting gap below  $T_c$ . This distinction could be achieved through the study of nonequilibrium relaxation dynamics that may be quite different even for excitations with overlapping frequencies.

Previous time-domain studies of the lattice and carrier dynamics in  $\text{YBa}_2\text{Cu}_3\text{O}_{7-\delta}$  have already revealed changes on a subpicosecond scale close to  $T_c$ . In the superconducting state, the coherent amplitude of the Ba phonon mode starts to grow [5,6] and a strong increase in the relaxation time is observed [7–9]. Both anomalies were linked to the breaking of Cooper pairs, even though they are described within different theoretical approaches—the dispersive excitation of coherent phonons [10] and changes of the Drude tail, modification of matrix elements, and a two-fluid model for the nonoscillatory part of the ultrafast response [7–9,11]. Moreover, a few studies performed on underdoped samples showed that the characteristics of the pseudogap can be observed in the time domain [12–14]. Guided by these experimental and theoretical developments, we have undertaken a thorough time-domain study to elucidate the uniformity of the pseudogap state. In this Letter we report (1) the existence of two crossover temperatures above  $T_c$ , which are identified through an abrupt modification of both the lattice and carrier dynamics on a subpicosecond scale and (2) a hysteresislike behavior for these crossovers, indicative of competing ground states.

As a sample we used a  $c$ -axis-oriented film of  $\text{YBa}_2\text{Cu}_3\text{O}_{7-\delta}$  grown by off-axis laser deposition on  $\langle 100 \rangle$  MgO. The film is 350 nm thick and has a superconducting transition at  $T_c = 88$  K. In Raman spectroscopy the sample exhibits a softening of the  $340 \text{ cm}^{-1}$  mode (by  $\approx 4 \text{ cm}^{-1}$ ), which proves that the doping is close to the optimum, since for underdoped  $\text{YBa}_2\text{Cu}_3\text{O}_{7-\delta}$  no softening is observed [15]. The time-resolved data

and Raman spectra obtained in different regions of the film revealed no measurable difference, which testifies to the homogeneity of the sample.

The film was mounted on the cold finger of an optical cryostat and the excitation and detection of reflectivity transients were carried out with a degenerate pump-probe setup. In the pump-probe experiment the pump beam excites the carriers and the delayed probe pulse beam monitors the reflectivity change  $\Delta R(t)$  as a function of the delay time between the two beams. We employed a Ti:sapphire mode-locked laser operating at 780 nm and delivering a 78 MHz train of 50 fs pulses. These pulses were divided into high-intensity pump and low-intensity probe pulses polarized perpendicular to each other. The average power ratio of the pulses was 30:1, with the probe power not exceeding 3 mW. Both the pump and probe beams were kept close to normal incidence and focused to a spot diameter of 350  $\mu\text{m}$ . The corresponding temperature increase of the sample is estimated to be less than 2–3 K.

Typical transient reflectivity changes for  $\text{YBa}_2\text{Cu}_3\text{O}_{7-\delta}$  are shown in Fig. 1(a). There is a pulse-limited increase of the reflectivity on the order of  $10^{-4}\Delta R/R_0$  at  $t = 0$  and a subsequent relaxation back to equilibrium. The transient at positive time delay consists of two contributions: an oscillating signal, due to the excitation of coherent phonons, superimposed on a nonexponentially decaying signal due to electronic excitation. The nonoscillatory decay consists of a fast and a slow component as can be seen from the plots in logarithmic scale shown in Fig. 1(a). At longer decay time ( $> 10$  ps), the relaxation becomes increasingly longer. This decay appears, for certain temperatures, at negative time delays, stemming from incomplete signal decay between successive laser pulses. Given the repetition rate of 78 MHz, the slow signal decays on a nanosecond scale.

As far as temperatures well below and far above  $T_c$  are concerned we observe a behavior similar to previous time-domain experiments. At room temperature the relaxation time of the overall signal is close to 0.5 ps and the tiny oscillations, superimposed on the decaying signal, correspond to the coherent  $A_g$  phonon (4.6 THz) generated by the Cu displacement. At helium temperature, the relaxation time is modified and the oscillations are dominated by the  $A_g$  phonon (3.7 THz) generated by the Ba displacement. In addition to the two  $A_g$  phonons observed earlier [5,6], for helium temperature we observe for the first time the coherent excitation of the  $B_{1g}$ -like mode centered at 10 THz and the Raman-forbidden mode at 7.2 THz; see Fig. 1(b). However, in this study we are primarily interested in the ultrafast response above  $T_c$ , and we use the superconducting behavior as a reference for the comparison to the normal state behavior. The series of transients in Fig. 2(a) illustrate the temperature dependence of the ultrafast optical response. Below  $T_c$ , the relaxational dynamics is dominated by the slow relaxation within 3–5 ps. With increasing temperature,  $(\Delta R/R_0)_{\text{max}}$  decreases [7,8,11,12]; however, the temperature dependence of  $(\Delta R/R_0)_{\text{max}}$  in

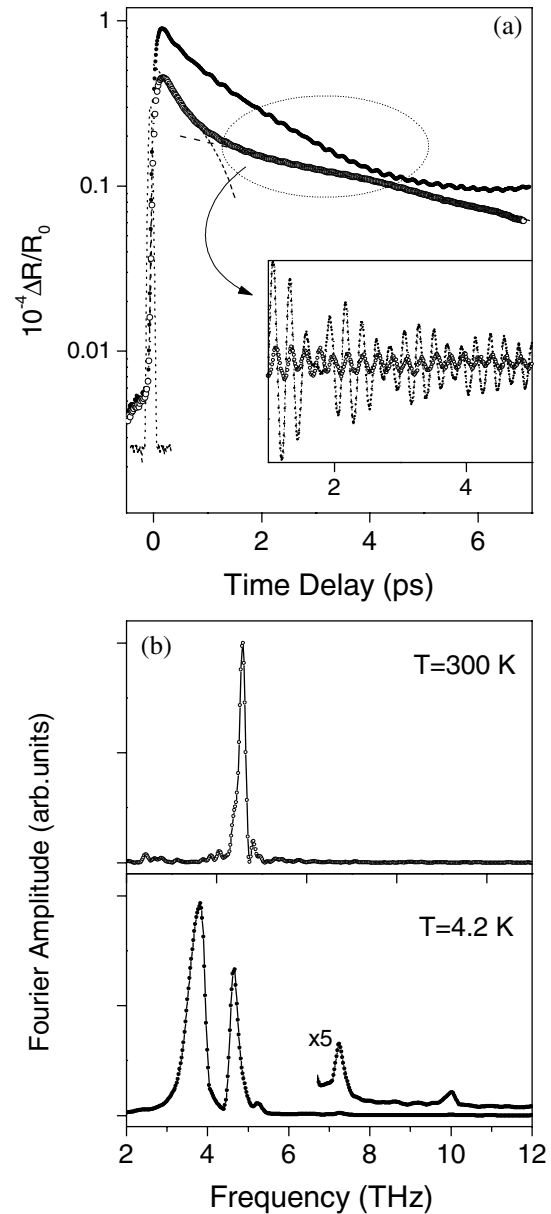


FIG. 1. (a) Transient differential reflectivity  $\Delta R(t)/R_0$  versus time delay at 300 K (open circles) and 4 K (closed circles) on a logarithmic scale to emphasize the fast and slow components of the transients, both indicated by dashed lines for the room temperature transient. The laser autocorrelation signal is shown by a dotted line. The inset depicts enlarged oscillatory components. (b) Fourier transformed (FT) spectra of the oscillatory component.

the superconducting state follows neither the BCS nor the two-fluid model behavior, as shown in Fig. 3 [16]. The ratio of the Ba/Cu amplitudes in the FT spectra also decreases as the temperature approaches  $T_c$ ; see Fig. 2(b). Above  $T_c$ , this ratio is reduced almost to zero [17]. However, at around 160 K the initial differential reflectivity changes  $\Delta R/R_0$  reverses sign, and the ratio of Ba/Cu amplitudes jumps to its helium temperature value. The main difference from the superconducting state is that the differential reflectivity, reduced to a spike, has the

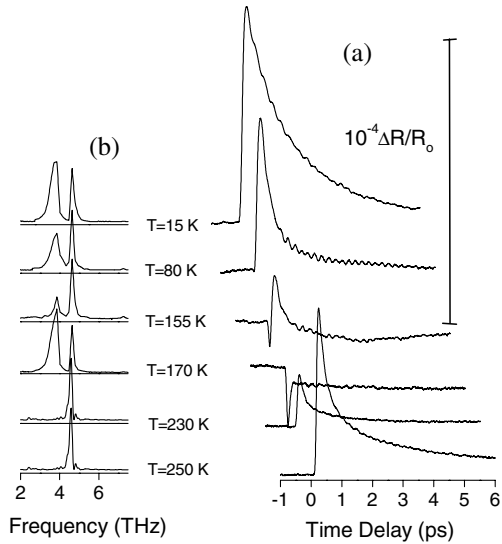


FIG. 2. (a) The transient differential reflectivities  $\Delta R(t)/R_0$  (offset horizontally and vertically for clarity) and (b) normalized FT spectra of the oscillating parts of  $\Delta R(t)/R_0$ , obtained for different temperatures on the way from the superconducting to the normal state.

opposite sign. These features both of the lattice and carrier dynamics continue approximately up to 220 K and then again, the sign of  $(\Delta R/R_0)$  is changed, and the Ba mode vanishes from the transients. In a limited temperature range around  $T_1^*$  and  $T_2^*$  the transients are of mixed type with both positive and negative components, whereas within the  $T_1^*-T_2^*$  range the signal consists of a time-resolution limited spike and an electronic component not decaying on a ps time scale.

It is most remarkable that the temperatures  $T_1^*$  and  $T_2^*$ , which border the regime with slow carrier dynamics and altered lattice dynamics in the metallic state, exhibit a

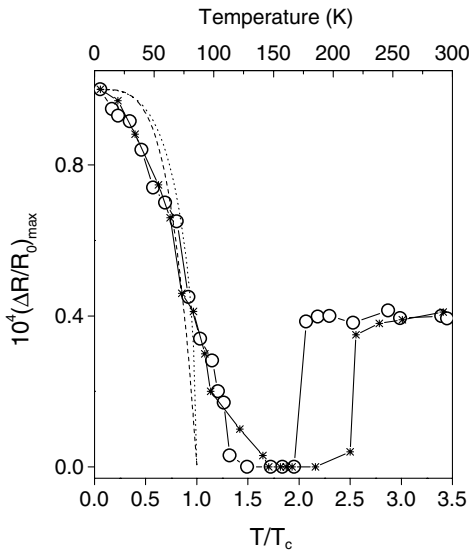


FIG. 3.  $(\Delta R/R_0)_{\max}$  as a function of temperature: open circles, decreasing temperature; stars, increasing temperature. Dotted and dashed lines depict, respectively, the BCS and two-fluid model temperature dependence of the order parameter.

hysteretic behavior. When approaching the superconducting transition from above, their values ( $T_1^* \approx 175$  K,  $T_2^* \approx 115$  K) are different from those attained for crossing  $T_c$  from below ( $T_1^* \approx 220$  K,  $T_2^* \approx 160$  K). For the nonoscillatory response this can be seen from Fig. 3 and for the lattice contribution this memory effect is illustrated by the ratio of Ba/Cu amplitude as a function of temperature, shown in Fig. 4. In both cases, one can see that there is no hysteresis for the superconducting state: the ratios and maximal differential responses are the same for increasing and decreasing temperatures. The lack of a hysteresis in the superconducting state where non-negligible signals at negative time delays are most pronounced [11] can be taken as evidence that accumulation effects are not responsible for the hysteresis. Moreover, the data taken at a lower excitation density (30% in comparison to the data presented in Figs. 3 and 4) revealed that the temperatures  $T_1^*$  and  $T_2^*$  characterizing the hysteresis do not depend on the excitation density. On the other hand, the large amount of hysteresis in the pseudogap state suggests that the transition into this state might be a first order phase transition.

We are not able at present to provide a full description of the nonequilibrium dynamics of the lattice and carriers; nevertheless, we will try to summarize the most important facts that may help in doing this. The ultrafast relaxation dynamics in  $\text{YBa}_2\text{Cu}_3\text{O}_{7-\delta}$  have been explained within the model for displacive excitation of coherent phonons [10]. Two experimental facts question this description; first, the lack of a cosine dependence for the phase of coherent phonons observed in femtosecond experiments [5,6] and, second, the excitation of  $B_{2g}$  ( $B_{3g}$ ) off-diagonal coherent phonons in  $\text{YBa}_2\text{Cu}_3\text{O}_{7-\delta}$  crystals, which are not expected to be excited by the displacive mechanism [18]. These two observations may point to a Raman-like mechanism for the coherent phonon excitation

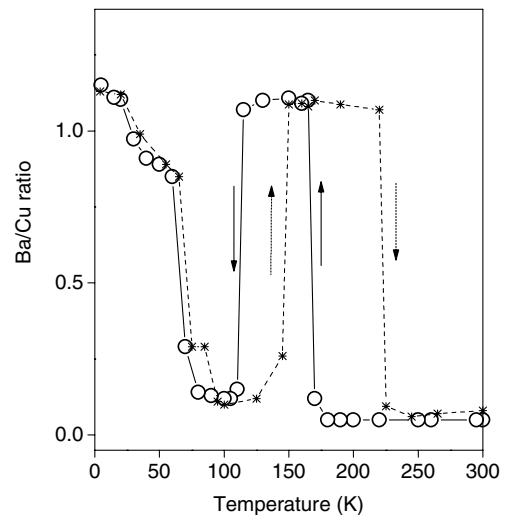


FIG. 4. Temperature dependence of the Ba/Cu intensity ratio from the FT spectra. Arrows indicate the direction of temperature change: open circles, decreasing temperature; stars, increasing temperature.

[19]. Obviously, the identification of the mechanism for coherent phonon generation is a prerequisite for the interpretation of the peculiar dependence observed in our pump-probe study. In this respect we mention the hysteretic behavior observed in spontaneous Raman scattering for optimally doped crystals of  $\text{YBa}_2\text{Cu}_3\text{O}_{7-\delta}$  [20]. It consisted of an enhancement of odd-parity phonon modes for the  $yy$  polarization at an electric quadrupole or magnetic dipole transition. This enhancement can be bleached at helium temperature by irradiating the crystal with  $h\nu > 2.2$  eV photons; however, on the way back to room temperature the modes emerge again in the temperature range 180–220 K. The frequency for one of the modes matches exactly the frequency of the Raman-forbidden mode observed in our time-domain experiment at helium temperature. The intermediate state for scattering was identified as having  $B_{3g}$  symmetry and a lifetime of the order of 10 fs [20]. A rough estimate for the lifetime of the state responsible for the negative polarity spike is 30 fs. The connection between the hysteresis observed in Raman and the memory effect in the time domain is not clear. If such a relation exists, the origin of the hysteresis can be linked to CuO chains. To clarify the connection, time-resolved experiments on untwinned crystals are needed.

The nonuniform pseudogap regime has been theoretically considered as coming from (i) local pairing and itinerant behavior of the electron pairs [3], (ii) weak and strong pseudogap regimes for a nearly antiferromagnetic Fermi-liquid [2], or (iii) the formation of charge inhomogeneities (stripe fluctuations) and the onset of superconductivity on individual stripes [4]. Our present results do not strongly favor any of these interpretations. Some features of the observed temperature behavior can readily be explained within a particular model, whereas others cannot be accounted for. For example, the existence of the slowly decaying component (indicative of a localized nature of the excitation) in the temperature range  $T_1^* - T_2^*$  may be taken as evidence of the onset of local pair formation, whereas its disappearance as the local pairs becoming itinerant. The coherent phonon spectra in the  $T_1^* - T_2^*$  range being similar to those in the superconducting spectra support such an explanation. However, in the  $T_2^* - T_c$  range, where the pairs are presumably itinerant, the coherent phonon spectra are quite similar to those observed for temperature above the upper crossover temperature  $T_1^*$ . Why the itinerant but noncoherent pairs are decoupled from the lattice remains unclear. Still, the similarity of coherent lattice dynamics in the superconducting and pseudogap states encourages us to suggest that electron-phonon coupling is necessary to explain the data. Alternatively, the upper crossover temperature can be ascribed to the onset of a weak pseudogap regime where hot spots in the Fermi surface start to appear, whereas the low crossover temperature can be taken as the beginning of a strong pseudogap regime where the Fermi surface starts losing its pieces. However, there is no place for the lattice in this near antiferromagnetic Fermi-liquid picture since

the coupling of hot quasiparticles to the lattice is presumably weak [2].

In summary, we have reported the existence of three distinct crossover temperatures in nearly optimally doped  $\text{YBa}_2\text{Cu}_3\text{O}_{7-\delta}$ . One is the superconducting transition temperature  $T_c$ , and two other temperatures,  $T_1^*$  and  $T_2^*$ , are found at  $T > T_c$ . At these temperatures both the carrier and lattice dynamics are radically altered. These facts point to a nonuniform pseudogap regime of the phase diagram. The data presented in this study pose a new challenge to the theories attempting to describe the pseudogap. The most striking finding of our experiments is the observation that the crossovers in the pseudogap regime exhibit a hysteresislike behavior. Hopefully, this feature will allow singling out a correct theoretical model for the pseudogap state.

This work was supported by the Alexander von Humboldt Foundation (Germany) and the Russian Foundation for Basic Research (Grant No. 2000-02-16480).

- 
- [1] For a review, see T. Timusk and B. Statt, *Rep. Prog. Phys.* **62**, 61 (1999).
  - [2] J. Schmalian, D. Pines, and B. Stojkovic, *Phys. Rev. B* **60**, 667 (1999).
  - [3] P. Devillard and J. Ranninger, *Phys. Rev. Lett.* **84**, 5200 (2000).
  - [4] V.J. Emery *et al.*, *Phys. Rev. B* **56**, 6120 (1997).
  - [5] W. Albrecht, Th. Kruse, and H. Kurz, *Phys. Rev. Lett.* **69**, 1451 (1992).
  - [6] O. V. Misochko *et al.*, *Phys. Rev. B* **61**, 4305 (2000).
  - [7] S. G. Han *et al.*, *Phys. Rev. Lett.* **65**, 2708 (1990).
  - [8] G. L. Eeasley *et al.*, *Phys. Rev. Lett.* **65**, 3445 (1990).
  - [9] D. H. Reitze *et al.*, *Phys. Rev. B* **46**, 14 309 (1992).
  - [10] I. Mazin *et al.*, *Phys. Rev. B* **49**, 9210 (1994).
  - [11] C. J. Stevens *et al.*, *Phys. Rev. Lett.* **78**, 2212 (1997).
  - [12] J. Demsar *et al.*, *Phys. Rev. Lett.* **82**, 4918 (1999).
  - [13] R. D. Averitt *et al.*, *Phys. Rev. B* **63**, 140502 (2001).
  - [14] R. A. Kaindl *et al.*, *Science* **287**, 470 (2000).
  - [15] E. Altendorf *et al.*, *Phys. Rev. B* **47**, 8140 (1993).
  - [16]  $(\Delta R/R_0)_{\max}$  is determined here as the maximum of the positive reflectivity change.
  - [17] The Fourier transformation was carried out for the same time interval, since the ratio of components is a function of time delay for a two-mode spectrum [6]. In order to obtain the same interval we restricted the lower limit to approximately 1 ps, which could give some underestimate of the Ba amplitude.
  - [18] O. V. Misochko, *Zh. Eksp. Teor. Fiz.* **119**, 285 (2001) [*J. Exp. Theor. Phys.* **92**, 246 (2001)].
  - [19] Note, however, that the description of coherent phonon generation through the Raman-like mechanism has problems of its own. For example, the relative intensities in Raman and FT spectra are different [6]. This is most clearly seen when comparing the spectrum of Fig. 1 to the typical Raman  $yy$  spectrum (see Ref. [20]) in which the  $B_{1g}$  mode dominates.
  - [20] D. R. Wake *et al.*, *Phys. Rev. Lett.* **67**, 3728 (1991).